

STRUCTURAL SIGNATURE AND EXHUMATION P-T-T PATH OF THE GORGONA BLUESCHIST SEQUENCE (TUSCAN ARCHIPELAGO, ITALY)

Federico Rossetti*, Claudio Faccenna*, Laurent Jolivet**, Renato Funicello*, Bruno Goffé***, Francesca Tecce*, Christophe Brunet**, Patrick Monié** and Olivier Vidal***

* Dipartimento di Scienze Geologiche, Università, Largo San L. Murialdo 1, 00146-Roma, Italy, fax +39-06-54888201 (e-mail: rossetti@uniroma3.it).

** Département de Géotectonique, Université Pierre et Marie Curie, 4 Place Jussieu, 75252 Paris cedex 05, France.

*** Laboratoire de Géologie, Ecole Normale Supérieure, 24 rue Lhomond, 75231 Paris cedex 05, France.

* Centro di Studio per il Quaternario e l'Evoluzione Ambientale, C.N.R., Dipartimento di Scienze della Terra, Università la Sapienza, Piazza Aldo Moro, 1- Roma, Italy.

** Laboratoire de Géochimie et de Géochronologie, UMR 55-67, USTL-Université de Montpellier II, Montpellier, France.

Keywords: blueschist metamorphism, (Fe, Mg)-carpholite, "Schistes Lustrés" Nappe, P-T-t paths, fluid inclusions, syn-orogenic extension. Northern Tyrrhenian Sea.

ABSTRACT

In this paper we present a study on the metamorphic and structural evolution of the Gorgona Island, located in the Northern Tyrrhenian Sea. Based on their contrasting P-T histories, two major tectonic units bounded by a mylonitic contact are recognised. The lower one (CS Unit) shows typical HP/LT parageneses (Fe-carpholite and glaucophane); peak metamorphic conditions are estimated around 1.5 GPa at temperature lower than 350°C. A Late Oligocene (25±0.3 Ma) age is proposed for this blueschist event on the basis of ⁴⁰Ar/³⁹Ar geochronology on phengites. The upper unit (Oph Unit) contains parageneses representative of the blueschist-greenschist transition; peak metamorphic conditions are estimated around 0.6-0.8 GPa and at least 300°C. Therefore, a normal-sense metamorphic gap is observed across the mylonitic contact (in the order of 0.7 GPa), with pressure increasing towards the lower CS Unit. Eastward asymmetric ductile shear, syn-kinematic relative to the retrograde greenschist stage, accompanied exhumation of the CS Unit, controlling the contact with the upper Oph Unit. On the basis of both structures and metamorphic history, the contact between the two units may be thus considered as an extensional detachment. The good preservation of carpholite and the absence of retrograde chloritoid below the shear zone show that exhumation of the CS Unit occurred along a cooling, nearly isothermal path. We link this retrogressive evolution to a syn-orogenic extensional unroofing mechanism connected to the dynamics of the Northern Apennine-Alpine Corsica orogenic wedge.

INTRODUCTION

The Northern Apennine orogeny is the result of a long convergence history between the European and the Adriatic continental domains from Late Cretaceous to Tertiary (e.g., Dal Piaz, 1974; Principi and Treves, 1984; Dewey et al., 1989; Bortolotti et al., 1990; Lahondère, 1996). The intervening oceanic units, belonging to the Ligurian-Piedmont domain, were progressively deformed and accreted to the continental margins, with the formation of a double-verging orogenic wedge, consisting of the westward verging Alpine Corsica system and the eastward verging Apennines one (Principi and Treves, 1984; Jolivet et al., 1998a). In the Northern Tyrrhenian region (Fig. 1), occurrence of HP/LT index minerals both in continental- and oceanic-derived units suggests a continuity of HP/LT metamorphism moving from Alpine Corsica (Fournier et al., 1991; Lahondère, 1996) to Tuscany (Ricci, 1972; Theye et al., 1997; Giorgetti et al., 1998; Rossetti et al., 1999). Peak metamorphic pressure estimates decrease eastwards from 2.0 to 0.6 GPa at temperatures between 250° and 450°C (Jolivet et al., 1998a and references therein). Eastward asymmetric ductile extension accompanied exhumation of these HP/LT units under LT conditions, suggesting a mechanism of extension contemporaneous with the formation of the Northern Apennine accretionary complex (Jolivet et al., 1998a).

The aim of this paper is to describe the metamorphic and structural evolution of the oceanic-derived, blueschist "Schistes Lustrés" sequence exposed on the Gorgona Island (Fig. 1), and its relationships with the tectonic evolution of the Northern Tyrrhenian region. Limiting metamorphic min-

eral equilibria, fluid inclusion and structural analysis tools were used in order to constrain the thermal and tectonic evolution that accompanied the exhumation of these rocks. In addition, a preliminary ⁴⁰Ar/³⁹Ar geochronological study was performed on a "Schistes Lustrés" sample, representing the first radiometric age obtained from the metamorphic units of the Gorgona Island. These data add new insights on the accretionary evolution of the Northern Apennine chain, and on the tectonic interpretation of this region.

GEOLOGICAL SETTING

Due to its location, the Gorgona Island (Fig. 1) represents the physiographical link between Alpine Corsica and the Tuscan region. The island is an isolated fragment of the oceanic-derived "Schistes Lustrés" Nappe and is composed by two main tectonic units, separated by a sharp, NW-SE trending, steep mylonitic contact (Mazzoncini, 1965) (Fig. 2). The lower unit (CS) mainly consists of metapelites (quartz-albitic micaschists) and metapsammites in association with carbonatic levels (calcschists and marbles, *Mar*), transitional to coarser-grained rocks at the base of the unit (*Mcl*) (Mazzoncini, 1965; Capponi et al., 1990). The CS Unit shows an important HP/LT signature (see below). The upper unit (*Oph*) consists of an ophiolitic complex, made of serpentinites and metamorphosed basic rocks, mostly equilibrated at greenschist-facies metamorphic conditions (Mazzoncini, 1965). Nevertheless, occurrence of Na-amphibole in metabasites (Capponi et al., 1990) suggests an incipient low-grade blueschist metamorphism. In the upper part of the

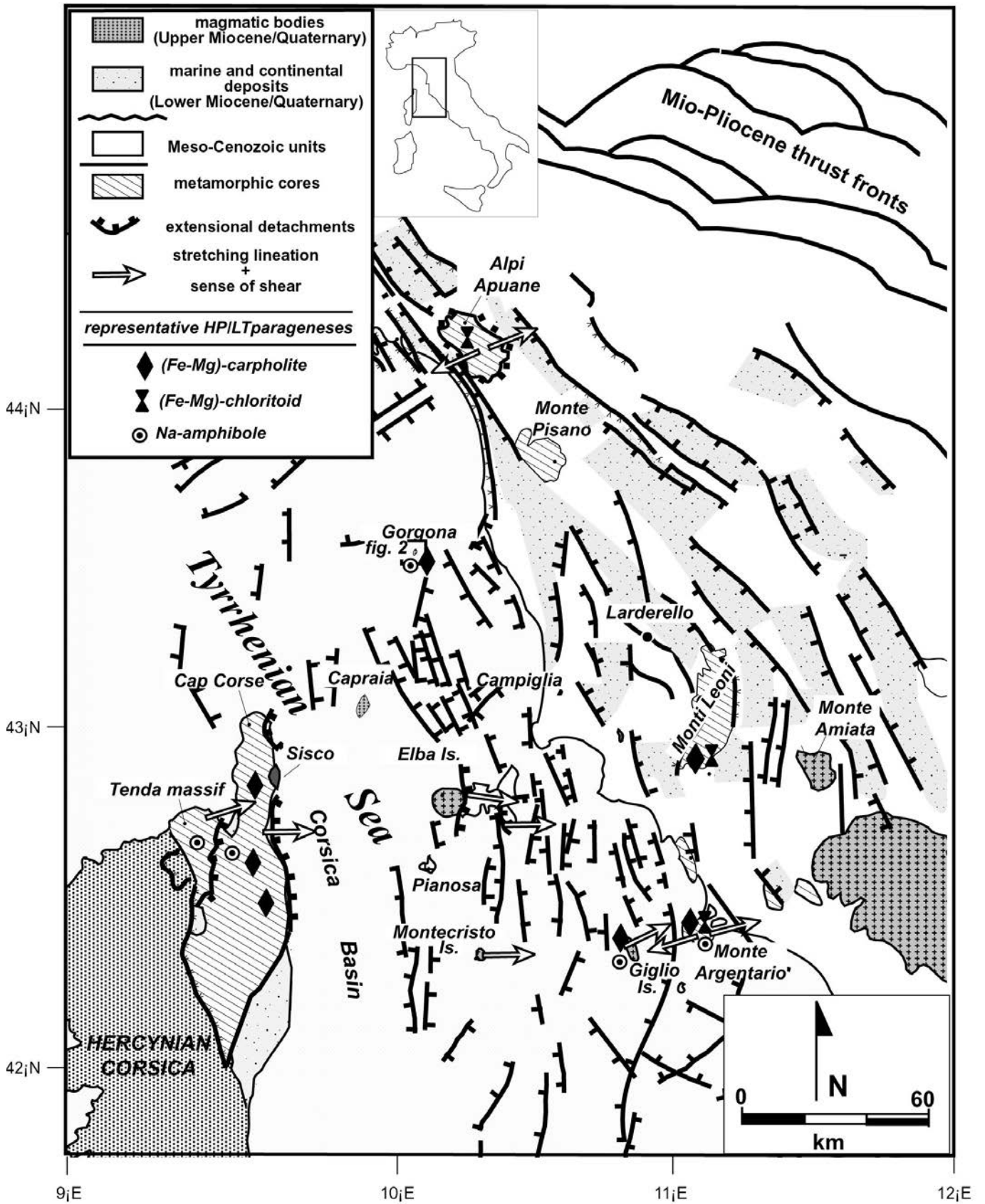


Fig. 1 - Simplified tectonic map of the Northern Apennines-Northern Tyrrhenian Sea region. The studied area is squared (modified after Jolivet et al., 1998a)

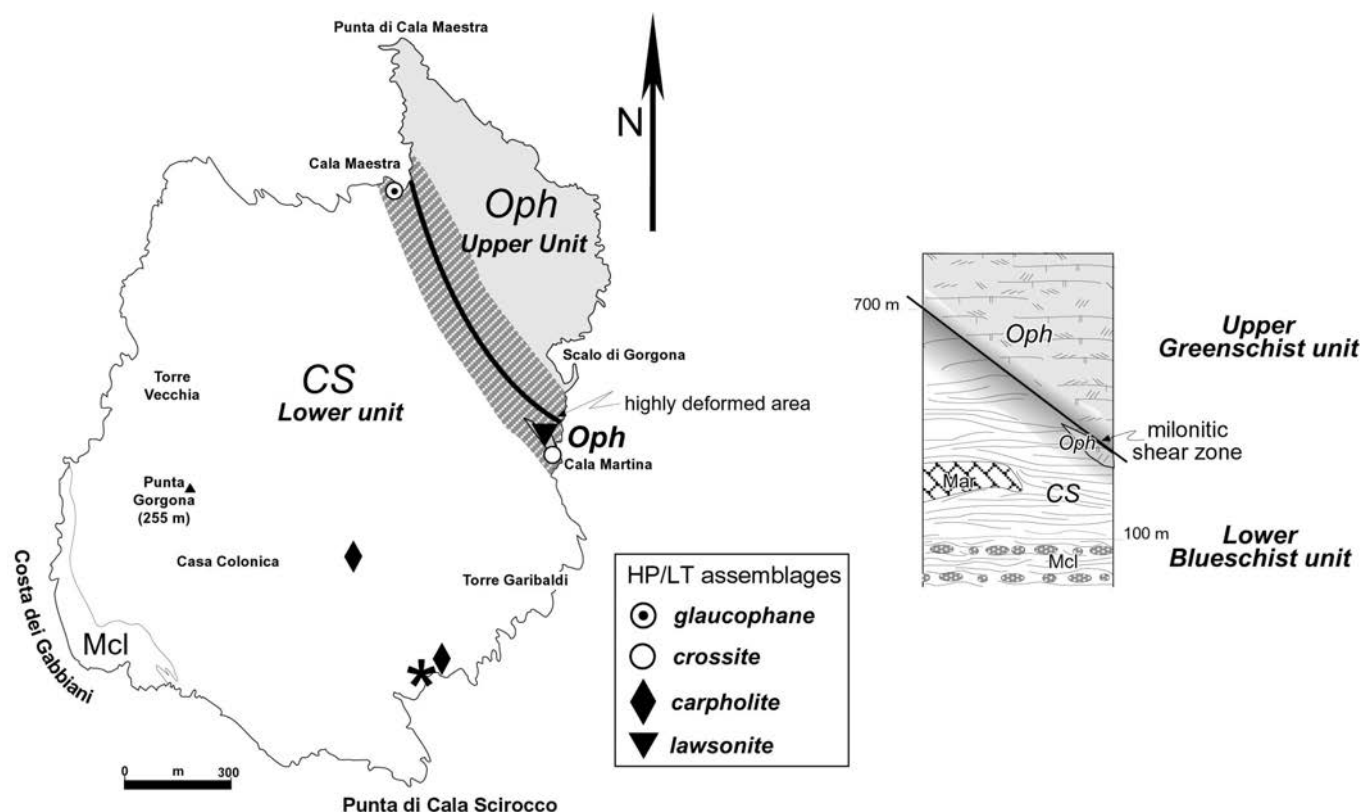


Fig. 2 - Geological map of the Gorgona Island (modified after Mazzoncini, 1965 and Capponi et al., 1990) and schematic columnar section showing the relationships among the exposed units; occurrence of HP/LT minerals are also shown. *Oph*- serpentinites and greenschist facies basic rocks; *CS*- ("Schistes Lus-trés" Unit), calcshists, minor marbles (*Mar*) and basal coarser-grained rocks (*Mcl*). Star indicates sample location for the radiometric study.

CS Unit, tectonic slices of *Oph* metabasic rocks are also present (see the tectono-stratigraphic column in Fig. 2).

Structural analysis performed by Capponi et al. (1990) pointed out a major second-stage deformation event, interpreted as related to overthrusting of the *Oph* Unit onto the *CS* one, along the mylonitic contact.

METAMORPHIC EVOLUTION

Parageneses and mineral compositions

To estimate the P-T metamorphic conditions, mineral phase relations and compositions were examined for limit-

ing equilibrium associations in both metapelitic *CS* and metabasic *Oph* rocks. The *CS* Unit contains HP/LT associations, such as (Fe, Mg)-carpholite (reported in the following as carpholite *s.l.*) + chlorite + phengite + quartz in metapelites and Na-amphibole + chlorite + quartz in mafic schists. Conversely, in the upper *Oph* Unit greenschist parageneses are ubiquitous and include albite + chlorite + epidote + tremolite, in association with lawsonite and albite in metagabbros. Locally blue-amphibole crystals are observed in a chlorite-epidote matrix. No evidence for lawsonite in equilibrium with blue-amphibole has been detected. The different parageneses for both the tectonic units are summarised in Fig. 3.

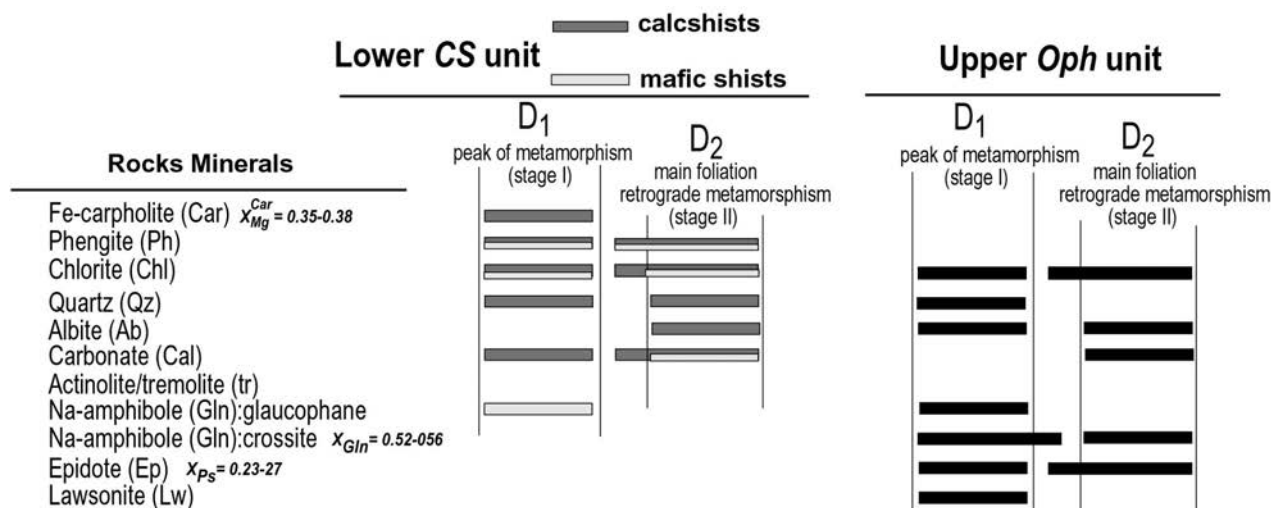


Fig. 3 - Sequence of deformation and main parageneses occurring in the tectonic units of the Gorgona Island.

The mineral analyses were obtained using a Cameca SX50 electron microprobe (operating conditions: 15 kV, 15nA, 20 s counting time) and mineral formulae were calculated on the basis of number of oxygen per anhydrous formula (see Tables 1 and 2).

CS Unit

The main constituents of the metapelitic matrix are quartz, phengite, calcite, abundant albite and chlorite; additional minerals may be paragonite, tourmaline, apatite, Fe-oxides, zircon (Mazzoncini, 1965). These minerals are seldom accompanied by green columnar aggregates of carpholite fibres, which occur as vein-filling minerals in synfolial segregations of quartz (Fig. 4a). Presence of carpholite testi-

fies for an important low-grade HP metamorphic imprint (see e.g. Oberhänsli et al., 1995; Jolivet et al., 1998b and references therein). Carpholite is usually well preserved and is found in a simple textural equilibrium with chlorites and phengites. Only locally, carpholite phenoblasts are replaced by fine-grained aggregates of phyllosilicates (white micas \pm chlorite) and albite. No chloritoid has been found and no evidence for the presence either of kaolinite or pyrofillite in equilibrium with carpholite has been detected. In Na-rich levels, the HP/LT imprinting is attested by the occurrence of idiomorphic blue amphibole crystals, coexisting with chlorite and white micas (Fig. 4b). The main rock fabric consists of a second-stage crenulation cleavage defined by folding of the carpholite + quartz + phengite composite associations,

Table 1 - Representative microprobe analyses and structural formulae of minerals in equilibrium during the peak of metamorphism in the CS Unit

	<i>calcshists</i>						<i>mafic schists</i>				
	Carpholite		Phengite	Chlorite			Phengite	Chlorite	Na-amphibole ²		
SiO ₂	69.53	58.83	50.06	49.43	23.88		51,37	51,76	27,85	56,97	55,94
TiO ₂	0	0	0.08	0.10	0.02		0,11	0,11	0	0,08	0,14
Al ₂ O ₃	15.13	20.96	27.47	29.39	22.87		24,83	25,21	18,39	9,48	10,65
FeO	7.42	9.75	3.03	2.32	29.93		3,71	2,80	21,25	16,74	12,99
MnO	0.23	0.49	0	0.05	0.08		0,09	0	0,16	0,30	0,19
MgO	2.36	2.98	2.46	2.03	10.25		3,98	3,98	18,79	6,68	7,87
CaO	0	0	0.02	0.03	0.03		0,20	0,22	0,27	0,29	1,85
Na ₂ O	0	0	0.19	0.25	0		0,69	0,19	0,03	6,92	6,81
K ₂ O	0	0	10.22	10.01	0		9,50	10,54	0,02	0,04	0,07
F	0.19	0.37	0	0.83	0		0,12	0	0	0	0,25
—	94.86	93.38	93.53	94.44	86.06		94,60	94,81	86,76	97,50	96,76
Cations	80x.		110x.		140x.		110x.		140x	230x.	
Si	3.57	3.06	3.40	3.34	2.62		3,47	3,48	2,89	8,01	7,94
Ti			0	0.01	0		0,01	0,01	0	0,01	0,01
Al	1.93	1.96	2.20	2.34	2.87		1,98	1,99	2,26	1,57	1,78
Fe ³⁺	0.07 ¹	0.03 ¹	0.17	0.13	2.75		0,21	0,16	1,85	0,40	0,11
Fe ²⁺	0.60	0.61							0,01	0,57	1,43
Mn	0.02	0.03	0	0	0.08		0,01	0	2,92	0,04	0,02
Mg	0.38	0.35	0.25	0.20	1.68		0,40	0,40	0,03	1,40	1,66
Ca			0	0	0		0,01	0,02	0	0,04	0,13
Na			0.02	0.03	0		0,09	0,02	0,01	1,90	1,87
K			0.89	0.86	0		0,82	0,90	0	0,01	0,01
F	0.06	0.09	0	0.15	0		0	0		0	0,11
XMg	0.38	0.35			0.38				0.61	0.69	0.53

X_{Mg} in minerals is calculated as X_{Mg} = Mg/(Mg+Fe+Mn).

¹ Fe³⁺ calculated as equal to 2-Al.

² Following the recalculation of Robinson et al. (1982), sodic amphiboles analyses are normalised on the basis of 13 cations, excluding Ca, Na, and K.

Table 2 - Representative microprobe analyses and structural formulae for the mafic rocks of the *Oph* Unit

<i>Oph unit</i>						
	Na-Amphibole ¹		Epidote		Chlorite	
SiO ₂	56.91	56.52	38.30	41.29	27.48	
TiO ₂	0.04	0.2	0.98	0.15	0.08	
Al ₂ O ₃	6.46	6.05	24.53	22.43	18.26	
FeO	17.85	17.65	10.45	11.14	22.23	
MnO	0.11	0.13	0.22	0.09	0.19	
MgO	9.14	9.04	0.05	0.08	18.66	
CaO	0.88	0.84	23.37	21.75	0.10	
Na ₂ O	6.79	6.78	0.01	0	0	
K ₂ O	0.02	0.02	0	0	0	
F	0	0	0	0.18	0	
—	98.20	97.23	97.91	97.11	87.00	
Cations	23Ox.		25Ox.		14Ox.	
Si	7.94	7.98	6.15	6.63	2.87	
Ti	0	0.02	0.12	0.02	0.01	
Al	1.06	1.01	4.64	4.25	2.25	
Fe ³⁺	1.05	0.89	1.40	1.49		
Fe ²⁺	1.12	1.19			1.945	
Mn	0.01	0.01	0.03	0.01	0.02	
Mg	1.95	1.90	0.01	0.02	2.902	
Ca	0.13	0.13	4.02	3.74	0.01	
Na	1.81	1.85	0.02	0.09	0	
K	0	0			0	
F	0	0	0		0	
XMg	0.63	0.61	XPs	0.23	0.27	XMg
XGl	0.55	0.52				g

Activity models according to Evans (1990).

¹ Following the recalculation of Robinson et al. (1982), sodic amphiboles analyses are normalised on the basis of 13 cations, excluding Ca, Na, and K.

attesting that growth of the carpholite-bearing segregations represents an early event in the metamorphic history (Fig. 4a). Textural relations indicate that various amounts of plastic deformation post-dated the HP/LT stage with the crystallisation of retrogressive association of calcite + albite + chlorite ± white micas. Calcite crystals are strongly deformed, with thick twins. Calcite usually contains inclusions of carpholite, phengite, chlorite and Na-amphibole.

Representative chemical analyses of the main mineral phases are listed in Table 1. X_{Mg} of carpholites ranges between 0.35 and 0.38 (Fe-carpholite) and the fluorine content is relatively low (around 0.2-0.3 wt%). The mean Si^{4+} content of phengites in equilibrium with carpholites varies between 3.34 and 3.40 a.p.f.u., and chlorites show an average X_{Mg} of 0.38. Blue amphibole compositions mostly plot in the glaucophane field (Fig. 5) and Si^{4+} contents up to 3.53 a.p.f.u. are reported for phengites in equilibrium with Na-amphibole.

Oph Unit

The studied metabasites occur as tectonic slices at the top of the *CS* Unit, in the highly strained contact area with the

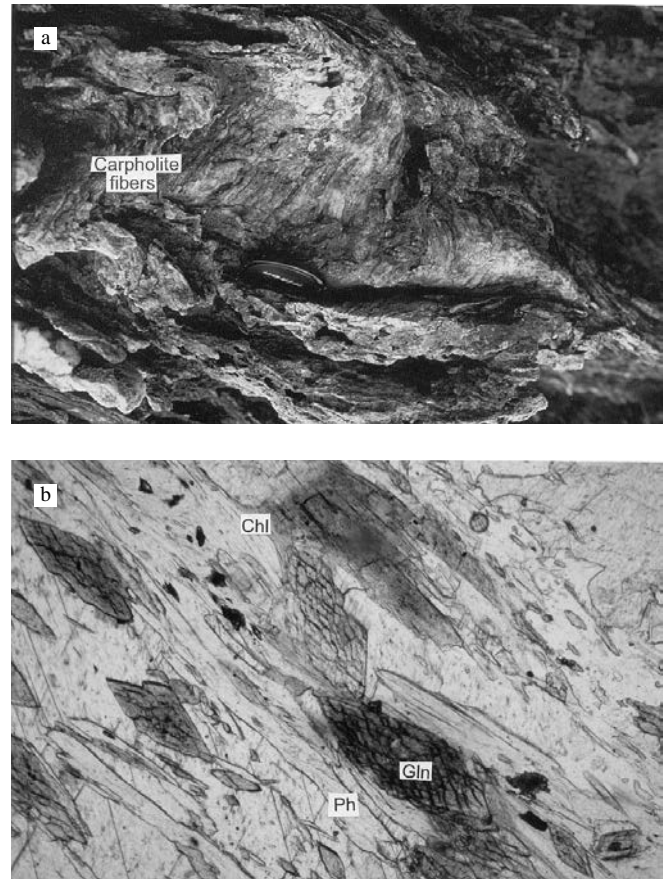


Fig. 4 - Representative HP index minerals in the lower *CS* Unit. (a) Fresh Fe-carpholite fibers in association with quartz in the *CS* metapelites (exposure near Cala Scirocco in Fig. 2; lens cap for scale); (b) Thin section showing glaucophane (gln) crystals coexisting with chlorite (Chl) and phengite (Ph) included in late calcite crystals (Cala Maestra in Fig. 2; natural light; horizontal width 1.5 mm).

upper *Oph* Unit (see the tectonic stratigraphic section in Fig. 2). The metabasic rocks mainly derived from volcanic precursors and are dominated by greenschist-facies metamorphic assemblages. This lithological association is chiefly composed of layered metabasites consisting of blueschist and chlorite-epidote alternations. The matrix of the *Oph* rocks is composed of epidote grains along with chlorite, albite and tremolite. Pristine igneous assemblages are represented by augitic clinopyroxene, plagioclase and calcic amphibole (Mazzoncini, 1965; Capponi et al., 1990). Blueschist facies metamorphic assemblages occur within a relict foliation along the greenschist schistosity and consist of blue amphibole and chlorite-epidote composite associations. The greenschist-facies re-equilibration is usually associated with a mylonitic texture reworking the early blueschist associations with syn-kinematic crystallisation of albite + chlorite + calcite + epidote ± actinolite-tremolite. Relict blue amphibole and/or lawsonite crystals are often present as armoured inclusions in epidote or albite and more frequently in calcite-rich parageneses. Compositions of the mineral phases representative of the metamorphic parageneses observed in the *Oph* Unit are presented in Table 2. Na-amphibole compositions plot within the crossite field (Fig. 5) and show X_{Gl} [= X_{Al}^{VI}] ranging between 0.52 and 0.54. Epidote shows no evidence of compositional variations for both epidotes in equilibrium with blue amphibole and in the retrogressed matrix; the pistacite content [$X_{Ps} = Fe^{3+}/(Al+Fe^{3+})$] varies between 0.23 and 0.27.

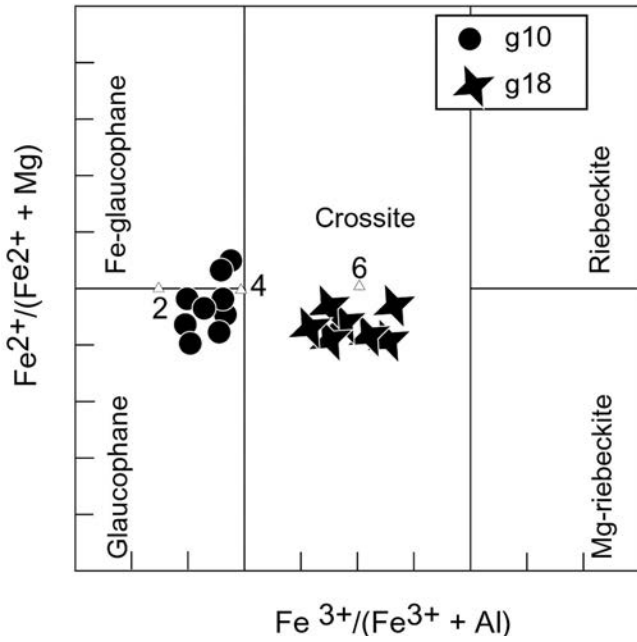


Fig. 5 - Composition of Na-amphibole occurring in both the CS (g10) and *Oph* (g18) Units. Classification after Miyashiro (1957). Numbers refer to the compositions of Evans (1990).

P-T estimates and exhumation trajectories

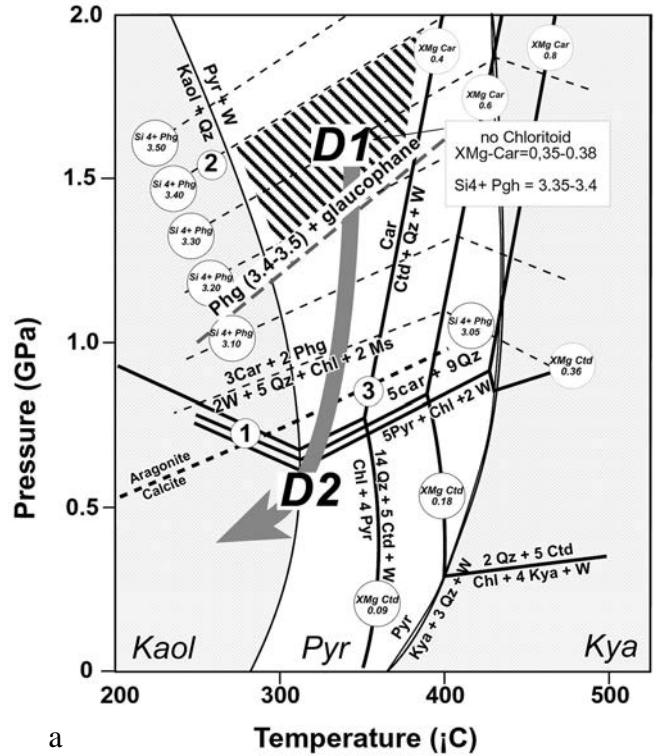
Occurrence of Fe-carpholite in the CS Unit and Na-amphibole in the *Oph* Unit metabasites indicates blueschist metamorphic conditions. To determine more precisely the peak P-T conditions relevant for the observed parageneses, mineral equilibria were calculated using the computer program PTAX, a recent development of GEO-CALC software of Berman and Perkins (1987), with the internally consistent dataset of Berman (1988), coupled with carpholite data from Vidal et al. (1992) and metabasite components from Evans (1990).

Mixing properties in phengites are based on the data of Massonne (1995) used in Oberhänsli et al. (1995) and Jolivet et al. (1998b).

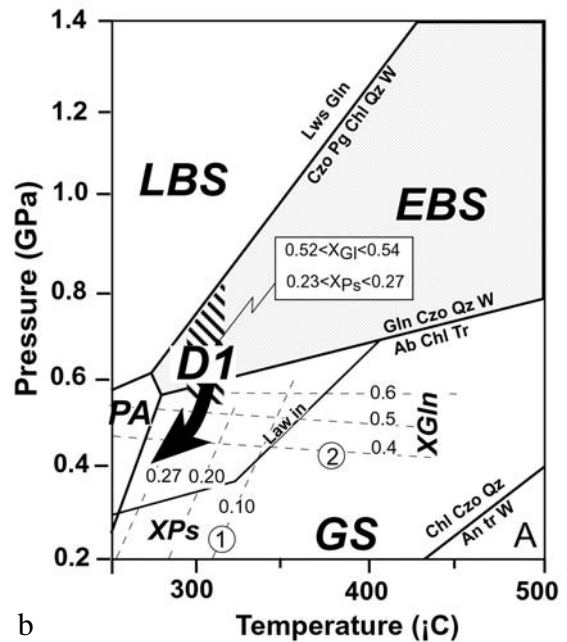
CS Unit

Presence of Fe-carpholite coexisting with phengite and chlorite and absence of chloritoid in metapelites allow for accurate determination of the peak P-T metamorphic conditions and of a possible P-T path during exhumation. (e.g. Fournier et al., 1991; Oberhänsli et al., 1995; Jolivet et al., 1996; Theye et al., 1997). Low-grade metapelites mineralogy is here referred to a synthetic P-T grid presented in Oberhänsli et al. (1995) and Jolivet et al., (1998b). In this grid (Fig. 6a), the association carpholite-phengite acts as a geobarometer through reaction (2), $3\text{carpholite} + 2\text{celadonite} = 2\text{H}_2\text{O} + 5\text{quartz} + \text{chlorite} + 2\text{muscovite}$, which describes the progressive change of the phengitic substitution in white micas in equilibrium with carpholite; the association carpholite-chloritoid acts as geothermometer, as carpholite is rapidly destabilised in chloritoid through reaction (3), $\text{carpholite} = \text{H}_2\text{O} + \text{quartz} + \text{chloritoid}$, with $X_{\text{Mg-car}}$ increasing with temperature (Chopin and Schreyer, 1983; Vidal et al., 1992).

In the Gorgona samples chloritoid is absent, and consequently reaction (3) yields only maximum temperatures, in the order of 350°C ($X_{\text{Mg-car}} = 0.4$, Fig. 6a). The lack of evidence for kaolinite or pyrophyllite in equilibrium with the HP/LT assemblages did not allow us to provide further indications on the thermal conditions during the peak of meta-



a



b

Fig. 6 - Estimated P-T conditions and exhumation paths for the different units of the Gorgona Island. (a) Conditions derived from the Fe-carpholite bearing CS Unit using the P-T grid proposed in Oberhänsli et al. (1995) and Jolivet et al. (1998b). Thick lines represent the major reactions in the FMASH system involving carpholite, chlorite, chloritoid and quartz. The positions of these reactions depend upon the Fe/Mg ratio (X_{Mg}) in carpholite and chloritoid. Dotted lines represent various Si^{4+} a.p.f.u. contents of phengites in equilibrium with carpholites (reaction 2). Isopleth for phengites (Si^{4+} a.p.f.u. =3.45-3.50) in equilibrium with glaucophane is also shown (see text for further details). (b) Conditions derived for the *Oph* Unit (stability fields after Evans (1990): EBS- epidote-blueschist facies; GS- greenschist facies; LBS- lawsonite-blueschist facies; A- amphibolite facies, PA- pumpellyite-actinolite facies). Isopleths of constant composition of epidote X_{Ps} (1) and sodic amphibole X_{Gl} (2) for the blueschist and greenschist transition assemblages are after Maruyama et al. (1986). For mineral abbreviations see Fig. 3.

morphism. For temperatures lower than 350°C, pressures estimates through phengite substitution ($\text{Si}^{4+} = 3.34\text{-}3.40$) in white micas in equilibrium with carpholite indicate values ranging from 1.3 to 1.7 GPa (Fig. 6a). Note that pressure conditions determined using the phengite compositions co-existing with carpholite contain some uncertainties, as the muscovite-celadonite solid solution used here was derived from experiments conducted at temperature above 800°C (Massonne, 1995) and its extrapolation to lower temperature conditions has not been verified (see Jolivet et al., 1998b). These pressure estimates have thus to be considered as maximum estimates. Nevertheless, preliminary results concerning the prograde phengite-glaucophane-chlorite equilibrium for phengites of $3.45\text{-}3.5 \text{ Si}^{4+}$ a.p.u.f. show isopleths passing at 1.0 GPa-250°C and 1.4 GPa-350°C (Vidal and Trotet, pers. comm.), thus supporting metapelites geobarometry (Fig. 6a). This allowed us to propose peak pressure conditions in the order of 1.4-1.5 GPa for temperature lower than 350°C (Stage D₁ in Fig. 6a).

Because of the absence of chloritoid, the way back to the surface did not cross reaction (3) and thus remained along a cool gradient, attesting that the transition from blueschist to greenschist facies conditions did not involve any rise in temperature (Fig. 6a). In addition, the absence of preserved aragonite implies that the P-T conditions were under 0.5 GPa at 190°C (Gillet and Goffé, 1988), attesting a nearly isothermal retrograde path (Stage D₂ in Fig. 6a).

Oph Unit

P-T conditions for metabasites (Fig. 6b) were obtained from Na-amphiboles using the method of Evans (1990); crossite compositions are equivalent to composition 6 of Evans (1990) (see Fig. 5). The paragenesis found in these metabasites (chlorite, tremolite/actinolite, Na-amphibole, albite, epidote) is representative of the epidote-blueschist/greenschist-facies transition (see Maruyama et al., 1986). Because of the high variance of the system, the geothermobarometric estimates were also based on the isopleths of constant compositions of Na-amphibole (X_{Gl}) and epidote (X_{Ps}) (see Table 2), calculated by Maruyama et al. (1986 and references therein) for the blueschist and greenschist transition assemblages (Fig. 6b). We have therefore obtained (stage D1 in Fig. 6b) temperatures between 275° and 300°C ($X_{\text{Ps}}=0.23\text{-}26$, isopleths 1 in Fig. 6b) and pressures between 0.6 and 0.8 GPa ($X_{\text{Gl}}=0.52\text{-}0.54$, isopleths 2 in Fig. 6b). In some samples, preservation of lawsonite and albite in pristine igneous plagioclase testifies for a cool retrograde path (see e.g., Liou et al., 1985).

FLUID INCLUSION ANALYSIS

A fluid inclusion study was performed on quartz-carpholite segregations belonging to the HP/LT CS Unit. The analysed samples also contain white micas, chlorite and late calcite. All samples were chosen by textural and structural relationships to represent earlier generation of quartz segregation at each outcrop.

Quartz grains are intimately associated with carpholite, and textural evidence such as ondulose extinction and diffuse recrystallisation in quartz shows that this mineral was formed in the early stage of metamorphism. Fluid inclusions are so abundant that it is not always easy to define their origins and relationships. Rare “isolated” inclusions might be considered as primary, but most inclusions are aligned along

trails, attesting a secondary origin. Two major types of fluid inclusions have been observed and distinguished based on their morphologies. One group refers to bigger (up to 150 µm) inclusions which show post-trapping textures such as irregular dendritic and “explosion” textures (Fig. 7a and 7b). These inclusions were both empty and L+V. The second group contains smaller (up to 20 µm) inclusions aligned along trails, more evidently crosscutting each other and the grain boundaries. Inclusions in this group are secondary, L+V and show distinct negative-crystal-shaped textures (Fig. 7c). Calcite crystals host only this latter type of inclusions.

Microthermometric measurements were performed onto rock wafers polished on both sides using a Chaixmecha heating-freezing stage. Homogenisation temperatures and salini-

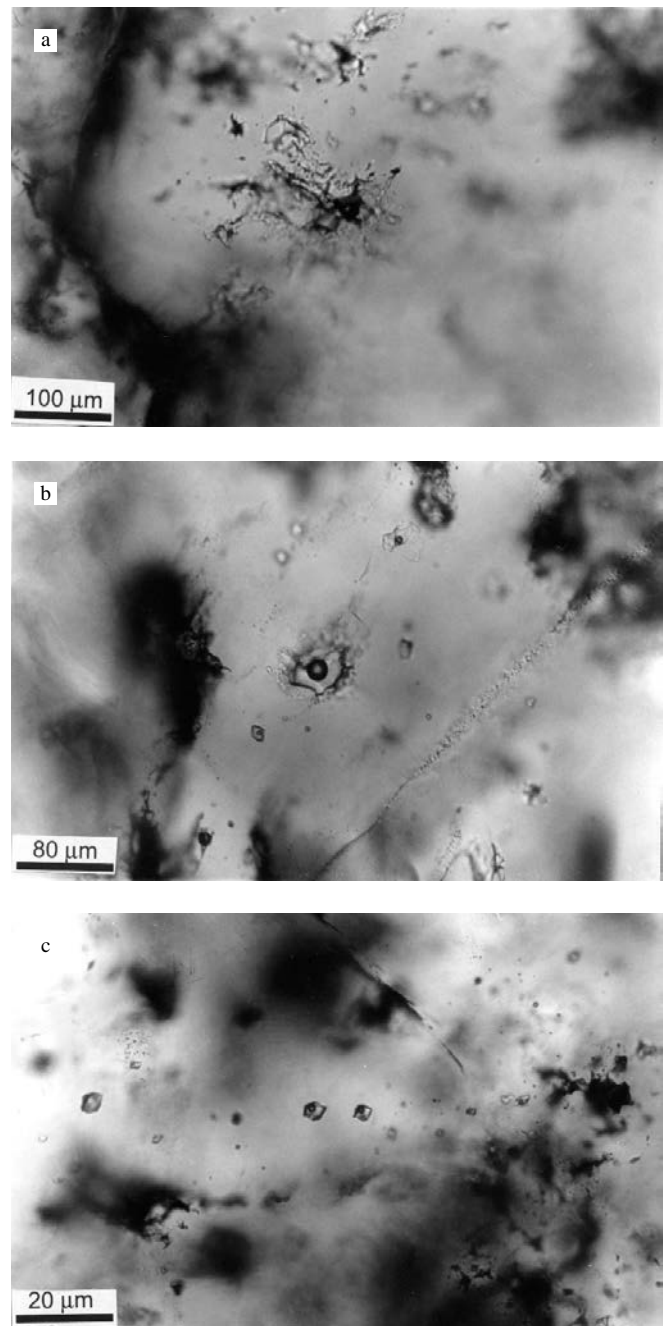


Fig. 7 - Photomicrographs of the different re-equilibration textures observed in fluid inclusions hosted in quartz grains associated with carpholite. (a) Highly irregular dendritic “exploded”. (b) Inclusion surrounded by “explosion” halos. Note to the left a plane of secondary smaller inclusions. (c) Plane of small secondary negative-crystal-shaped inclusions.

ties of the trapped fluid (Th) range from 150° to 200°C but mostly concentrate around 150° and 175°C for quartz, and around 175° and 200°C for calcite (Fig. 8a). Salinity values, resulting from the detection of the last melting temperature, are low in both cases (between around 2 and 5 wt% NaCl equivalent), although slightly higher in calcite (Fig. 8b). Higher values for both Th (from 175° to 200°) and salinity (around 9-wt% NaCl equivalent) occur in the bigger dendritic inclusions in quartz (Fig. 8a and 8b). The plot of Fig. 8c relates Th and salinities of the fluid trapped both in quartz and calcite grains; the little difference between the obtained values might indicate a possible moderate fluctuation of the temperature and composition of the fluid during time.

Results of experimental re-equilibration studies on synthetic fluid inclusions in quartz described the “explosion textures” as formed under conditions of internal overpressure due to unloading, and the intensity of the re-equilibration features depends on the magnitude of the internal overpressure and the size of the inclusions (e.g., Vityk et al., 1994; Vityk and Bodnar, 1995, and references therein). In particular, Vityk and Bodnar (1995) report that in experiments of isothermal decompression, low internal overpressure produces negative-crystal-shaped inclusions, while a much higher difference between internal and external pressure results in more evident morphological changes such as annular inclusions up to decrepitation clusters and explosion textures. Taking this

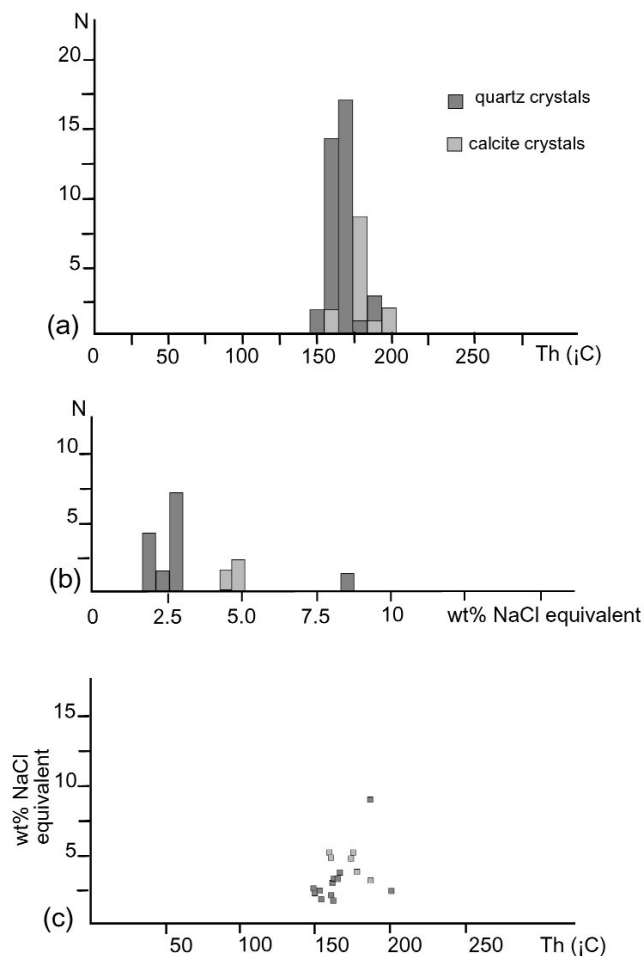


Fig. 8. (a) Histograms of homogenisation temperatures (Th) for secondary fluid inclusions in quartz (black) and calcite grains; data are superimposed (N number of analyses). (b) Histograms of salinity data (expressed in wt% NaCl equivalent) for inclusions as in (a). (c) Plot of Th vs. salinity data for the analysed inclusions.

into account, the differences among the re-equilibration morphologies of the fluid inclusions in quartz (highly dendritic and “explosion” textures) and in calcite (negative-crystal-shaped) possibly delineate a different record of the exhumation path associated to the CS Unit. Nevertheless, the similarity of microthermometric data for both minerals indicates that the fluid did not change very much in terms of salinity. Re-equilibration therefore occurred at thermal conditions around, and not higher than, 200°C, confirming that the retrogressive evolution for the CS Unit was rather cold.

DEFORMATION AND STRUCTURAL EVOLUTION

The reconstructed metamorphic evolution in the CS Unit is related to two main deformation events: D_1 , which was syn-kinematic relative to the HP/LT metamorphic stage and D_2 , syn- to post-kinematic relative to the greenschist retrogression.

D_2 deformation is strongly heterogeneous, bounding zones where D_1 structures are preserved. S_1 is defined by oriented glaucophane crystals in mafic schists and Fe-carpholite + quartz composite segregations in metapelites. Locally, the glaucophane crystals show a static growth, possibly indicating a polyphased HP metamorphic stage. Nevertheless boudinage of Na-amphibole crystals outlines a roughly N-S trending L_1 stretching lineation (Fig. 9).

The D_2 fabric mainly consists of a variably developed crenulation cleavage (S_2), which transposes the S_1 HP foliation, becoming the dominant foliation in zones of strong D_2 deformation. In particular, S_2 foliation is more penetrative, and intensity of the D_2 strain progressively increases moving towards the contact between the two tectonic units (Fig. 9). This zone is marked by a thick NW-SE oriented mylonitic shear zone. Within the mylonitic shear zone, the S_2 surfaces parallel the mylonitic foliation with the development of a S-L fabric. The L_2 stretching lineation, outlined by quartz/albite + chlorite in metapelites and epidote + albite in metabasites, constantly trends N120° (Fig. 9).

Synfolial D_2 folds re-fold the early HP assemblages (refer back to Fig. 4a) and are characterised by different folding styles moving from SW to NE across the island, with axes striking in various directions and clustering around NE-SW and WNW-ESE (Fig. 9). In zones of low D_2 strain, F_2 folds with NE-SW trending axes are gently recumbent and S_2 axial-planar surfaces form a discontinuous fracture cleavage (Fig. 10a). Intermediate zones of D_1 - D_2 superimposition show folding of the previous D_1 NNW-SSE oriented linear fabric, and development of a less ENE-WSW to ESE-WNW oriented L_2 mineral lineation. Approaching the contact with the upper *Oph* Unit, increase in the D_2 strain magnitude is attested by a change in the style of F_2 folds, which are mostly isoclinal with intense boudinage of the fold limbs (Fig. 10b). In the largest strain zones, these folds tend to rotate parallel to the N120° trending L_2 stretching lineation and decimeter-scale D_2 sheath folds are locally observed, as also suggested by Capponi et al. (1990). Kinematic indicators within the mylonitic zone, such as S-C structures, rotated clasts and asymmetric boudinage (e.g., Simpson and Schmidt, 1983) are associated with the greenschist parageneses (Fig. 10c) and indicate a constant top-to-the E-SE sense of shear or dextral-normal sense when the mylonitic foliation is steeper (Figs. 10c and 10d). Fold limbs are sheared out consistently with the overall eastward asymmetry of the D_2 deformation and rootless folds are usually ob-

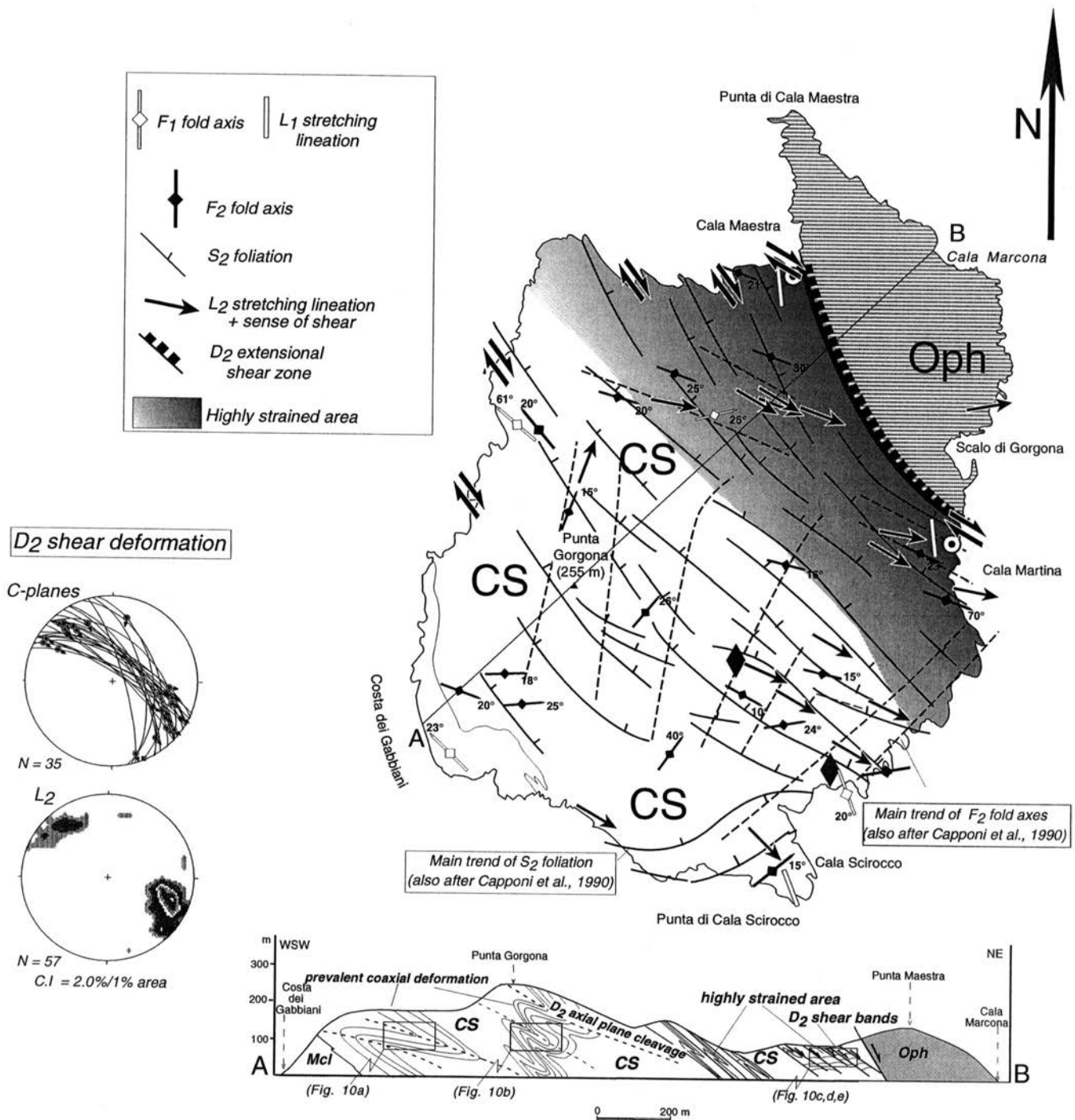


Fig. 9 - Structural map of the Gorgona Island (modified after Capponi et al., 1990) and schematic cross section showing the attitude of D_2 deformation. Stereoplots and contour diagrams (Schmidt equal-area projection, lower hemisphere) representative of the D_2 shear deformation are also shown.

served (Fig. 10e). Thus, the change in style and intensity of the D_2 strain moving towards the mylonitic contact is consistent with progressive shear deformation associated to a large amount of eastward-directed non-coaxial flow.

$^{40}\text{Ar}/^{39}\text{Ar}$ AGE OF THE HP-LT PARAGENESES IN THE CS UNIT

An $^{40}\text{Ar}/^{39}\text{Ar}$ geochronological study was performed on a sample (for location see Fig. 2) belonging to the metapelitic "Schistes Lustrés" CS Unit. This represents the first radiometric age from the metamorphic units of Gorgona Island.

A multi-grain population of phengites was separated from a metapelitic sample with well-preserved HP/LT assemblages (phengite + Fe-carpholite/quartz-rich segregations \pm chlorite). Phengites are usually highly substituted ($\text{Si}^{4+} = 3.30\text{-}3.40$) and carpholite is stable. $^{40}\text{Ar}/^{39}\text{Ar}$ ages were determined for the 80-100 μm size fraction prepared by setting methods from powdered specimens (see Weber, 1972, for sample preparation techniques). During this study, due to the fine-grained size of the micas, we used $^{40}\text{Ar}/^{39}\text{Ar}$ step heating of mineral bulk separates (≈ 100 mg) according to a classical analytical procedure (McDougall and Harrison, 1988; Maluski et al., 1990; Monié et al., 1994). Results are synthesised in Table 3 and presented as age spectra in

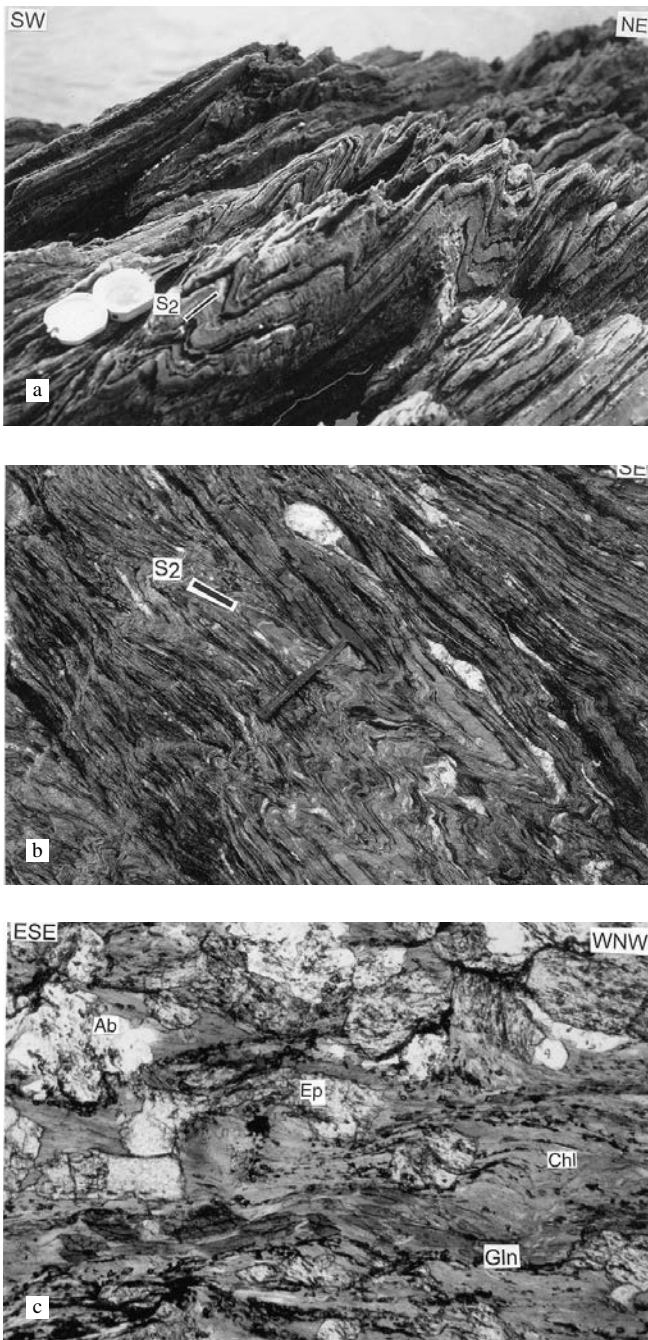


Fig. 11. Two sigma errors are reported. Only the errors on total ages and plateau dates include the uncertainty on the monitor age and its $^{40}\text{Ar}/^{39}\text{Ar}$ ratio.

The age spectra show a plateau date of 25.5 ± 0.3 Ma corresponding to 77% of the ^{39}Ar released and to an integrated date of 25.6 ± 0.3 Ma. An intercept age of 24.8 ± 0.3 Ma has been obtained in the $^{36}\text{Ar}/^{40}\text{Ar}$ vs. $^{39}\text{Ar}/^{40}\text{Ar}$ isotope correlation plot with an initial ratio of 452 ± 84 that is likely to be indicative of excess argon. Apparent ages increase up to 36 Ma at the end of the heating procedure that could be related to the presence of some impurities in the mineral separate.

As the analysed sample shows no retrogression in the greenschist facies, we conclude that that the obtained 25 Ma age is probably the age of the blueschist stage in Gorgona Island. This new preliminary result must be confirmed by further geochronological studies on highly retrograded samples, in order to further constrain the exhumation history of the blueschist sequence in Gorgona.

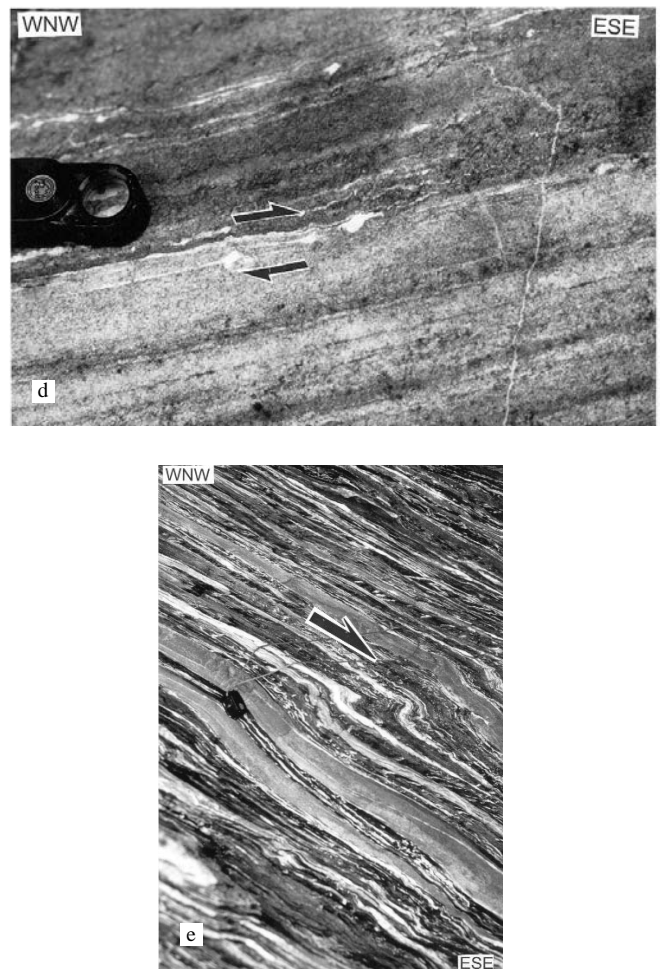


Fig. 10 - Aspect of the D_2 deformation in the CS Unit. (a) Spaced D_2 renuculation cleavage (exposure near Cala Scirocco in Fig. 9). (b) Isoclinal F_2 folds and D_2 boudinage in alternating beds of schists and quartzites. (c) Micro-scale top-to-the-ESE shear bands reworking an early HP foliation outlined by crossite (Gln) crystals and accompanying the greenschist retrogression in the Cala Martina metabasites; note the syn-kinematic crystallisation relative to the retrogressive stage of chlorite (Chl) + albite (Ab) + epidote (Ep) as outlined by opaque inclusion trails in epidote and albite crystals (section normal to S_2 and parallel to L_2 ; natural light). The horizontal width is 1.5 mm. (d) Asymmetric boudinage indicating top-to-the-ESE sense of shear in fine-grained mylonite at Cala Maestra (exposure parallel to L_2 and normal to S_2). (e) Eastward asymmetric F_2 folds and boudinage (top right) indicating top-to-the-ESE sense of shear within the D_2 mylonitic shear zone (exposure near Cala Martina in Fig. 9).

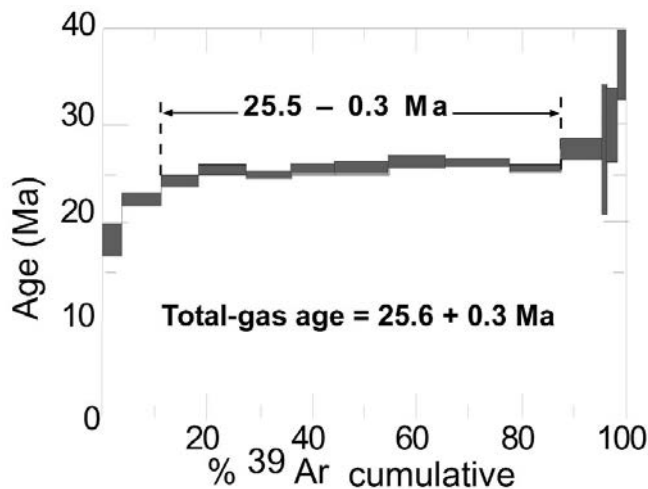
RELATIONS BETWEEN THE RECONSTRUCTED P-T-t PATHS AND THE TECTONIC EVOLUTION

Occurrence of Fe-carpholite and glaucophane with associated minerals (quartz, phengite \pm chlorite) is evidence of an early D_1 HP/LT imprinting in the lower CS (“Schistes Lustrés”) Unit, dated to the Late Oligocene by $^{39}\text{Ar}/^{40}\text{Ar}$ geochronology obtained on phengites. In Gorgona Island, the “Schistes Lustrés” sequence is similar to that cropping out in Alpine Corsica, where the blueschist parageneses gave older ages between 55 and 40 Ma ($^{39}\text{Ar}/^{40}\text{Ar}$ method on white micas: Lahondère, 1996; Brunet et al., 1997). As the Gorgona samples show no evidence of retrogression in the greenschist facies, we conclude that the HP event in Gorgona occurred later than in Corsica.

Unloading caused HP rocks to be progressively exhumed, resulting in pervasive overprinting at successively decreasing pressures, with a final re-equilibration at low-

Table 3 - Analytical data relative to the $^{40}\text{Ar}/^{39}\text{Ar}$ geochronology on the CS

GOR5	80-100 μm					
T ($^{\circ}\text{C}$)	$^{40}\text{Ar}/^{39}\text{Ar}$	$^{36}\text{Ar}/^{40}\text{Ar} \times 1000$	$^{37}\text{Ar}/^{39}\text{Ar}$	% Atm.	% ^{39}Ar	AGE $\pm 2\sigma$ (Ma)
500	0.605	2.527	0.139	74.6	0.8	31.44 \pm 4.64
50	0.839	1.936	0.029	57.2	0.9	43.41 \pm 29.18
600	0.347	1.118	0.075	33.0	3.5	18.13 \pm 1.57
650	0.429	0.483	0.067	14.2	10.9	22.36 \pm 0.55
680	0.466	0.279	0.002	8.2	18.1	24.24 \pm 0.55
710	0.488	0.383	0.000	11.3	27.3	25.39 \pm 0.48
740	0.479	0.241	0.000	7.1	36.1	24.95 \pm 0.46
770	0.488	0.242	0.002	7.1	44.6	25.41 \pm 0.49
820	0.492	0.347	0.001	10.2	54.6	25.59 \pm 0.62
860	0.502	0.485	0.001	14.3	65.3	26.15 \pm 0.58
900	0.503	0.476	0.001	14.0	77.6	26.19 \pm 0.49
950	0.490	0.461	0.002	13.6	87.7	25.53 \pm 0.46
1000	0.529	0.767	0.002	22.6	95.5	27.53 \pm 1.06
1050	0.529	2.064	0.000	61.0	96.4	27.54 \pm 6.58
1120	0.576	1.464	0.007	43.2	98.3	29.93 \pm 3.67
1200	0.696	2.433	0.032	71.9	100.0	36.13 \pm 3.57
						Total age = 25.6 \pm 0.3
						Plateau = 25.5 \pm 0.3

Fig. 11 - $^{40}\text{Ar}/^{39}\text{Ar}$ age spectra of single white mica grains from the CS Unit.

grade D_2 greenschist conditions. During exhumation and retrogression, two units with difference both in metamorphic grade and structural style were juxtaposed. The major conclusion is that a lower-P unit (*Oph*) rests in direct contact with a higher-P one (CS), attesting a normal-sense pressure gap (in the order of 0.7 GPa) across the mylonitic contact separating the two units. This evidence, coupled with the reconstructed sense of shear in the lower CS Unit, implies that the contact is an extensional shear zone, which moved the upper plate, represented by the *Oph* Unit, towards the E-SE. As a consequence, the second-phase deformation recorded in the CS Unit may be considered as the effect of thinning accommodated by the mylonitic shear zone.

The exhumation path of the Gorgona blueschist complex

is characterised by preservation of the Fe-carpholite-bearing assemblages, without any significant overprinting of the previous HP/LT assemblages. This is significant of an overall cool geotherm in the nappe pile during exhumation, in accordance with the homogenisation temperatures (around 200 $^{\circ}\text{C}$) of the fluid inclusions during the retrograde evolution. Exhumation thus likely occurred during convergence and further nappe stacking, in a way that preserved such a cool environment (e.g. Davy and Gillet, 1986). Extensional unroofing allowed the footwall rocks to be juxtaposed against cooler hanging wall rocks, while continuous underthrusting of cold units prevented significant heating during exhumation (e.g., Platt, 1986; Ernst and Peacock, 1996). Based on the above observations, a syn-orogenic style of extension is proposed for the top-to-the-E-SE shear post-dating the blueschist metamorphism of the Gorgona "Schistes Lustrés" CS Unit. The preliminary radiometric age determinations on the HP/LT stage in Gorgona thus represent further evidence for the eastward space-time migration of the compression-extension system within the inner Apennine Chain.

Acknowledgements

The authors wish to thank Dr. C. Mazzerbo who gave us the opportunity to work in the Gorgona Island. F.R. is grateful to R. Nicolas and M. Saracino for their help during microprobe analyses. The microprobe analyses were performed at the "Centro per la Geologia del Quaternario e la Geologia Ambientale", CNR-Roma. Thanks are due to an anonymous reviewer who provided helpful suggestions on an early version of the paper.

Financial support from ECC project n $^{\circ}$ EV5V-CT94-0464 ("Geodynamical modelling of an active region: the Apennines").

REFERENCES

- Berman R. G. and Perkins E. H., 1987. GEO-CALC: software for calculation and display of pressure-temperature-composition phase diagrams. *Am. Mineral.*, 72: 861-862.
- Berman R. G., 1988. Internally consistent thermodynamic data for minerals in the system $\text{Na}_2\text{O}-\text{K}_2\text{O}-\text{CaO}-\text{MgO}-\text{FeO}-\text{Fe}_2\text{O}_3-\text{Al}_2\text{O}_3-\text{SiO}_2-\text{TiO}_2-\text{H}_2\text{O}-\text{CO}_2$. *J. Petrol.*, 29: 445-522.
- Bortolotti V., Principi G. and Treves B., 1990. Mesozoic evolution of Western Tethys and the Europe-Iberia-Adria plate junction. *Mem. Soc. Geol. It.*, 45: 393-407.
- Brunet C., Monié P. and Jolivet L., 1997. Geodynamic evolution of Alpine Corsica based on new $^{40}\text{Ar}/^{39}\text{Ar}$ data. *Terra Nova Abstr.*, 9: 493.
- Capponi G., Giammarino S. and Mazzanti R., 1990. Geologia e morfologia dell'Isola di Gorgona. *Quad. Mus. Stor. Nat. Livorno*, 11: 115-137.
- Chopin C. and Schreyer W., 1983. Magnesiochloritoid and magnesiochloritoid: two index minerals of pelitic blueschists and their preliminary phase relations in the model system $\text{MgO}-\text{Al}_2\text{O}_3-\text{SiO}_2-\text{H}_2\text{O}$. *Amer. J. Sci.*, 283-A: 72-96.
- Dal Piaz G.V., 1974. Le metamorfisme alpin de haute pression et basse température dans l'évolution structurale du bassin ophiolitique alpine-apenninique. 1^e partie. *Boll. Soc. Geol. It.*, 93: 437-468.
- Davy P. and Gillet P., 1986. The stacking of thrust slices in collision zones and its thermal consequences. *Tectonics*, 5: 913-929.
- Dewey J.F., Helman M.L., Turco E., Hutton D.H.W. and Knott S.D., 1989. Kinematics of the Western Mediterranean. In: M.P. Coward, D. Dietrich and R.G. Park (Eds.), *Alpine tectonics*. *Geol. Soc. London Spec. Publ.*, 45: 265-283.
- Ernst, W.G. and Peacock S.M., 1996. A thermotectonic model for preservation of ultrahigh-pressure phases in metamorphosed continental crust. In: G.E. Bebout, D.W. Scholl, S.H. Kirby and J.P. Platt (Eds.), *Subduction: Top to bottom*. *A. G. U. Geophys. Monogr.* 96: 171-178.
- Evans B.W., 1990. Phase relations of epidote-blueschists. *Lithos*, 25: 3-23.
- Fournier M., Jolivet L., Goffé B. and Dubois R., 1991. Alpine Corsica metamorphic core complex. *Tectonics*, 10: 1173-1186.
- Gillet P. and Goffé B., 1988. On the significance of aragonite occurrence in the Western Alps. *Contr. Mineral. Petrol.*, 99: 70-81.
- Giorgetti G., Goffé B., Memmi I. and Nieto F., 1998. Metamorphic evolution of Verrucano metasediments in Northern Apennines: new petrological constraints. *Eur. J. Min.*, 10: 1295-1308.
- Jolivet L., Dubois R., Fournier M., Goffé B., Michard A. and Jourdan C., 1990. Ductile extension in Alpine Corsica. *Geology*, 18: 1007-1010.
- Jolivet L., Goffé B., Monié P., Truffert-Luxey C., Patriat M. and Bonneau M., 1996. Miocene detachment in Crete and exhumation P-T-t paths of high-pressure metamorphic rocks. *Tectonics*, 15: 1129-1153.
- Jolivet L., Faccenna C., Goffé B., Mattei M., Rossetti F., Brunet C., Storti F., Cadet J.P., Funicello R., Parra T. and D'Agostino N., 1998a. Mid-crustal shear zones in postorogenic extension: examples from the Northern Tyrrhenian Sea (Italy). *J. Geophys. Res.*, 103: 12,123-12,160.
- Jolivet L., Goffé B., Bousquet R., Oberhänsli R. and Michard A., 1998b. Detachment in high-pressure mountain belts, Tethyan examples. *Earth Planet. Sci. Lett.*, 160: 31-47.
- Lahondère D., 1996. Les schistes bleus et les éclogites à lawsonite des unités continentales et océaniques de la Corse Alpine. *Doc. B.R.G.M.*, 240, 285 pp.
- Liou J.G., Maruyama S. and Cho M., 1985. Phase equilibria and mineral parageneses of metabasites in low-grade metamorphism. *Min. Mag.*, 49: 321-333.
- Maluski H., Monié P., Kiénast J.R. and Rahmani A., 1990. Location of excess argon in granulitic facies minerals: a paired microprobe laser-probe $^{40}\text{Ar}/^{39}\text{Ar}$ analysis. *Chem. Geol.*, 80: 193-217.
- Maruyama S., Cho M. and Liou G.S., 1986. Experimental investigations of the blueschist-greenschist transition equilibria: pressure dependence of Al_2O_3 content in sodic amphiboles - A new geobarometer. *Am. Geol. Soc. Mem.*, 164: 1-16.
- Massonne H. J., 1995. Experimental and petrogenetic study of UHPM. In: R.G. Coleman and X. Wang (Eds.), *Ultrahigh pressure metamorphism, Cambridge topics in petrology*. Cambridge University Press, p. 33-95.
- Mazzoncini F., 1965. L'Isola di Gorgona. Studio geologico e petrografico. *Atti Soc. Tosc. Sci. Nat.*, 72: 185-237.
- McDougall I. and Harrison T.M., 1988. *Geochronology and thermochronology by the $^{40}\text{Ar}/^{39}\text{Ar}$ method*. Oxford University Press, New York, 212 pp.
- Miyashiro A., 1957. The chemistry, optics and genesis of alkali-amphiboles. *J. Fac. Sci. Univ. Tokyo*, 11: 57-83.
- Monié P., Torres-Roldan R.L. and Garcia Casco A., 1994. Cooling and exhumation of the western Betic Cordilleras, $^{40}\text{Ar}/^{39}\text{Ar}$ thermochronological constraints on a collapsed terrane. *Tectonophysics*, 238: 353-379.
- Oberhänsli R., Goffé B. and Bousquet R., 1995. Record of a HP/LT metamorphic evolution in the Valais zone: Geodynamic implications. In: B. Lombardo (Ed.), *Studies on metamorphic rocks and minerals of the western Alps*. Vol. in Memory of Ugo Pognante, *Boll. Museo Reg. Sci. Nat., Torino*, 13 (2): 221-239.
- Platt J.P., 1986. Dynamics of orogenic wedges and the uplift of high-pressure metamorphic rocks. *Geol. Soc. Am. Bull.*, 97: 1037-1053.
- Principi G. and Treves B., 1984. Il sistema corso-apenninico come prisma d'accrescimento. Riflessi sul problema generale del limite Alpi-Appennino. *Mem. Soc. Geol. It.*, 28: 529-576.
- Ricci C.A., 1972. Geo-petrographical features of the metamorphic formation of Tuscany. *Atti Soc. Tosc. Sci. Nat., Mem.*, 79: 267-279.
- Robinson P., Spear F., Schumacher J.C., Laird J., Klein C., Evans B.W. and Doolan B.L., 1982. Phase relations of metamorphic amphiboles: natural occurrences and theory. In: D. Veble and P.H. Ribbe (Eds.), *Amphiboles: Petrology and phase relations*. *Mineral. Soc. Am., Rev. Mineral.*, 9B: 1-211.
- Rossetti F., Faccenna C., Jolivet L., Funicello R., Tecce F. and Brunet C., 1999. Syn- versus post-orogenic extension: the case study of Giglio Island. (Northern Tyrrhenian Sea, Italy). *Tectonophysics*, 304: 73-92.
- Simpson C. and Schmid S.M., 1983. An evaluation of criteria to deduce sense of movement in sheared rocks. *Geol. Soc. Am. Bull.*, 94: 1281-1288.
- Theye T., Reinhardt J., Goffé B., Jolivet L. and Brunet C., 1997. Ferro- and magnesiochloritoid from the Monte Argentario (Italy): First evidence for high-pressure metamorphism of the metasedimentary Verrucano sequence, and significance for P-T path reconstruction. *Eur. J. Mineral.*, 9: 859-873.
- Vidal O., Goffé B. and Theye T., 1992. Experimental study of the stability of sudoite and magnesiochloritoid and calculation of petrogenetic grid for the system $\text{FeO}-\text{MgO}-\text{Al}_2\text{O}_3-\text{H}_2\text{O}$. *J. Metam. Geol.*, 10: 603-614.
- Vityk M.O. and Bodnar R.J., 1995. Textural evolution of synthetic fluid inclusions in quartz during reequilibration, with application to tectonic reconstruction. *Contrib. Mineral. Petrol.*, 121: 309-323.
- Vityk M.O., Bodnar R.J. and Schmidt C.S., 1994. Fluid inclusions as tectonothermobarometers: relations between pressure-temperature history and reequilibration morphology crustal thickening. *Geology*, 22: 731-734.
- Weber K., 1972. Notes on determination of illite crystallinity. *N. Jahrb. Geol. Pal. Mon.*, (6): 267-276.